



Assessing the fouling behavior of PTFE membrane in air-gap membrane distillation against oil-in-brine stabilized emulsions

Amr E. Mansi^{1,2} · Sahar M. El-Marsafy³ · Yasser Elhenawy^{2,4} · Mohamed Bassyouni^{1,2}

Received: 20 August 2023 / Accepted: 21 December 2023 / Published online: 28 January 2024
© The Author(s) 2024

Abstract

Understanding the fouling behavior in membrane operations is crucial for designing an effective treatment sequence. The membrane materials, feed characteristics, and operating conditions affect the fouling behavior. In this study, the fouling behavior of polytetrafluoroethylene (PTFE) membrane in membrane distillation was assessed after the treatment of oil-in-brine stabilized emulsions. Membrane backwash by water in membrane distillation partially restored the membrane's initial condition and eliminated salt fouling. Moreover, the effect of feed pretreatment by ultrafiltration on the fouling of the subsequent PTFE membrane was investigated. Remarkable improvements in salt rejection (> 98.5%) and oil rejection (> 96%) were observed for the hybrid system. Extensive characterizations were carried out to evaluate the fouling behavior. Surface morphology and elemental analysis revealed the nature of foulants. Fourier transform infrared spectroscopy was utilized to study the change in the surface chemistry of the membranes after being subjected to the oily brine feed. No peak shifting was observed indicating no chemical bonding between the organic contaminants and the membrane surface. Further elaboration of the results was achieved by measuring the mechanical stability and contact angle of the membranes. Reduction in the mechanical properties and water contact angle of the membranes was observed after fouling and wetting. Results indicated that ultrafiltration was an effective pretreatment process for membrane distillation using PTFE membrane. However, more unit operations should be incorporated to enhance the membranes' integrity.

Keywords Oilfield-produced water · Oily brine · Membrane wetting · Fouling

Introduction

Offshore oil and gas extraction activities increased tremendously in recent years. The importance of the oil extraction industry to the global economy cannot be overemphasized (Cai and Qin 2022). However, the environmental impact of the industry has reached a crucial level that cannot be overlooked any further (Devatha et al. 2019; Igwe et al.

2021). Various treatment processes were proposed for the treatment of oil-polluted brine (Saber et al. 2014; Elhady et al. 2020; Rahimi et al. 2020; Olajire 2020; Adetunji and Olaniran 2021; Falih et al. 2023). Membrane technologies were proven to be highly effective in handling such challenging feeds; yet, fouling persists as the major drawback of these technologies (Maddah et al. 2018; Ahmad et al. 2020; Mansi et al. 2022). Among the current membrane technologies, membrane distillation (MD) emerged as an efficient technique in the treatment of oil-polluted brine due to its high fouling resistance (Osman et al. 2019; Elhenawy et al. 2022a, b). Regarding the membrane distillation operation, wetting is another drawback that is exclusive to this technology (Sandid et al. 2021; Ye et al. 2023). The presence of a high concentration of soluble salts (e.g., sodium chloride) triggers scaling-induced wetting. Shi et al. 2022 systematically investigated the scaling formation and wetting progress in membrane distillation at high vapor fluxes. Results demonstrated that the scale layer proceeded in continuous motion until equilibrium. Initially, the high vapor

✉ Amr E. Mansi
amrmansi24@gmail.com; amr.elsayed@eng.psu.edu.eg

¹ Department of Chemical Engineering, Faculty of Engineering, Port Said University, Port Said, Egypt

² Center of Excellence in Membrane-Based Water Desalination Technology for Testing and Characterization (CEMTC), Port Said University, Port Said 42526, Egypt

³ Department of Chemical Engineering, Faculty of Engineering, University of Cairo, Giza, Egypt

⁴ Department of Mechanical Power Engineering, Faculty of Engineering, Port Said University, Port Said, Egypt

flux induced high concentration polarization, leading to rapid deposition of salts and pore blocking. The reduced flux due to pore blocking mitigated the concentration polarization effect and consequently led to the dissolution of the scale layer at the feed side. The regenerated pores served as a passage for salt molecules, leading to crystallization of salts within the pores ultimately transporting the wetting layer to the distillate side. Previous work investigated the interactions of oil-surfactant-brine systems in direct-contact membrane distillation (DCMD) (Han et al. 2017). When salt ions and sodium dodecyl sulfate surfactant co-existed in the solution, the ions enhanced the dissolution of the SDS in the aqueous phase consequently enhancing its mass transport to the vapor–liquid interface and intensifying membrane wetting. Pretreatment is therefore suggested to break the emulsion before membrane distillation operation. Ricceri, F. et al. utilized Fenton oxidation pretreatment to minimize the organic content of water before membrane distillation using polytetrafluoroethylene (PTFE) membrane (Ricceri et al. 2019). When the oil-polluted water was directly fed to the MD system, immediate wetting occurred which was evident by the escalation in permeate conductivity and water flux. The wetting mechanism was accelerated by the combined effects of foulants and the amphiphilic surfactant. A significant improvement was observed after Fenton oxidation; however, the total organic carbon content of the feed water remained roughly unchanged. Results indicate that the organic foulants were oxidized to a more hydrophilic and less foulant form rather than being completely decomposed. Other advised pretreatment options included floatation and ultrafiltration (Munirasu et al. 2016). Enhancing the hydrophobicity of the membrane aids in minimizing wetting. Functionalization of polyvinylidene fluoride membrane with SiO₂ enhanced the membrane hydrophobicity, liquid entry point, and porosity (Hamzah et al. 2018). The membrane flux was enhanced by 4 folds; however, salt and viscous emulsions deposited onto the membrane which deteriorated the flux. Other reports further elaborated on the enhancement of the intrinsic membrane properties by introducing omniphobic surfaces or the concept of Janus membranes (Huang et al. 2017; Mohammadi Ghaleni et al. 2018; Deka et al. 2019). A systematic study on the impact of feed composition and substrate wettability on wetting and fouling of Janus membranes in membrane distillation was conducted by (Kharraz et al. 2022). Three different feeds were tested in which the solvent was a 35 g/L NaCl solution. In the first case, SDS surfactant was added at a rate of 0.1 mM every 2 h, in the second case, 1000 ppm of oil was added to the solvent, and in the third case, both the oil and surfactant were added. The Janus membrane with a hydrophobic substrate and hydrophilic top layer started to suffer a severe drop in salt rejection in the first case at SDS concentration 0.3 mM. In the second case, mild wetting was observed,

and the salt rejection only dropped by 12% after 10 h. In the third case, the salt rejection dropped severely after the first 3 h. However, when a Janus membrane with an omniphobic substrate was used, the flux and salt rejection remained virtually unchanged in all the cases.

Numerous reports investigated the treatment of oil-polluted brines; yet, the investigation of the fouling behavior is limited in the literature. Therefore, this work is proposed to assess the fouling behavior on PTFE membrane in air-gap membrane distillation operation. The feed of brine and crude oil was prepared and tested in MD operation with and without pretreatment by ultrafiltration. In both cases, the fouling behavior was inspected in detail. Furthermore, the potential of the hybrid system in the treatment of the tested feed was evaluated.

Experimental

Materials

Polytetrafluoroethylene (PTFE) membrane was obtained from STERLITECH USA. The membrane characteristics as specified by the manufacturer are given in Table 1. PVDF pellets were purchased from Sigma-Aldrich. Crude oil was obtained from an offshore well in the Mediterranean Sea. Distilled water was obtained from GFL water still thermal distillation system (Conductivity ~ 3 μS/cm). Sodium chloride NaCl (99%) was purchased from MERCK. Potassium hydroxide KOH (85%) was purchased from Honeywell. Polysorbate 20 surfactant was purchased from MERCK.

PVDF membrane preparation and modification approach for ultrafiltration

Water pretreatment is essential for the stability of the membrane against oil-in-water emulsions. Therefore, the PVDF membrane was prepared according to the method described in (Mhlanga et al. 2014). The prepared PVDF membrane was then modified in a custom-made cell to decrease its water contact angle. The PVDF membrane

Table 1 Characteristics of the membrane utilized in this study

Membrane material	Polytetrafluoroethylene
Support layer material	Polypropylene
Average pore size	0.45 μm
Membrane porosity	65%
Membrane thickness	127 μm
Water contact angle	127°
Liquid entry pressure	0.76 bar

was dipped in a 4 Mole KOH /liter of distilled water for 2 h. The proposed reaction mechanisms for the PVDF membrane on polyester support are given in Eqs. (1) and (2). The membrane was assembled into a custom-made cell made of polymethyl methacrylate. The cell dimensions (Fig. 1) were 200 × 200 × 140 mm; however, it only contained a single square slot having dimensions of 120 × 120 × 70 mm. The modification cell was covered with a rubber gasket to prevent water evaporation from the solution during the reaction period. After the functionalization, the membranes were rinsed thoroughly with distilled water for 3 min to eliminate any trace of KOH. The resulting membrane was utilized to eliminate oil from the brine.

Membrane characterization

Surface morphology, average thickness, and autopsy of the pristine, functionalized, and tested membranes were acquired by using a TESCAN MIRA field-emission scanning electron microscope (FE-SEM) equipped with energy-dispersive X-ray spectroscopy (EDS) (OXFORD Xplore). The samples were dried and coated with 12 nm of gold/palladium alloy using Quorum mini sputter coater (SC7620) before imaging. EDS measurements were performed at 15 keV landing energy. Measurements were carried out on three different locations per sample and averaged.

The surface roughness of the pristine membrane was determined by atomic force microscopy (AFM) (Nanosurf

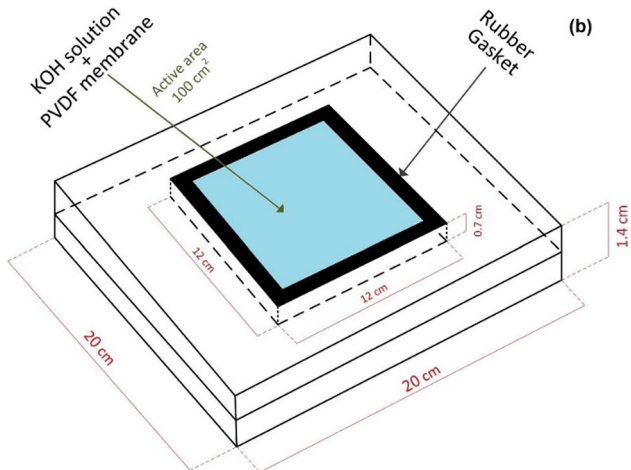
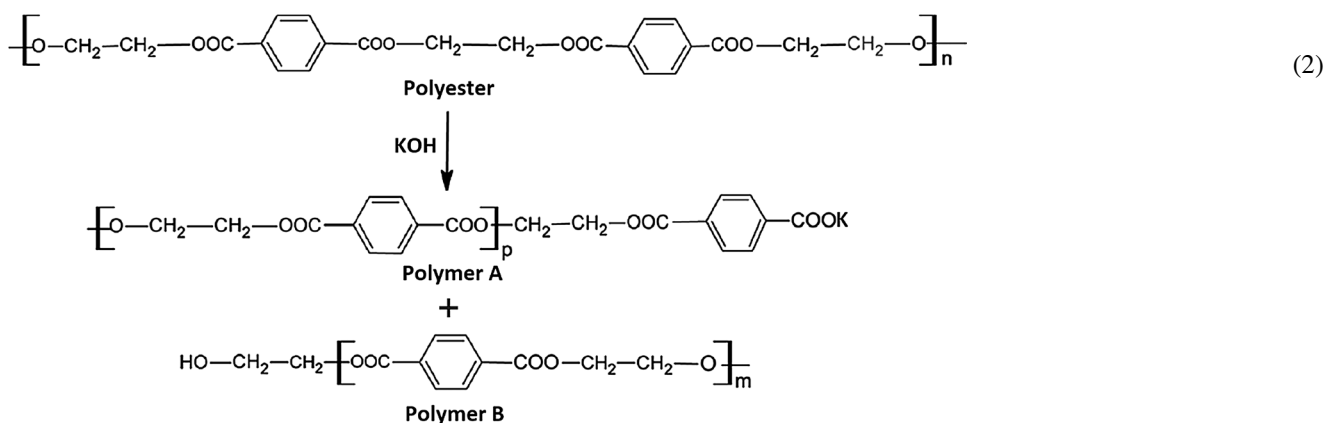
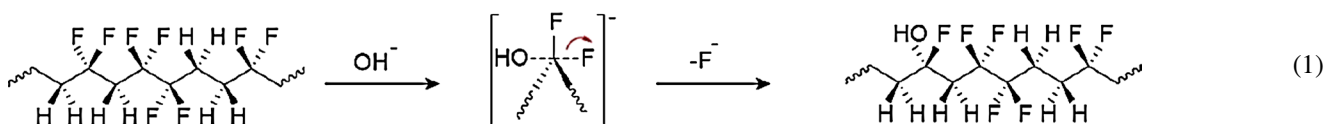


Fig. 1 Illustrative diagram of the cell utilized in PVDF membrane modification

FlexAFM). Measurements were performed in dynamic tapping mode using a 7 nm tip with a nominal resonant frequency of 190 kHz. Height data were recorded over a sample area of 225 μm².

Fourier transform infrared spectroscopy (FTIR) measurements were performed using BRUKER ALPHA II spectrometer equipped with an attenuated total reflection (ATR) platinum crystal. A total of 24 high-resolution scans were captured for each sample with a resolution of 4 cm⁻¹.

The water contact angles of the pristine and modified membranes were measured using an optical tensiometer. A 5 μL of DI water droplet was placed on the dried membrane samples. The measurements were performed at 20 °C on four random points on each sample and presented the data with one standard deviation.

The mechanical strengths of the pristine, modified, and tested membranes were tested by using a materials testing machine (Zwick/Roell Z1010). The membrane was cut into

2 × 8 cm strips and tested till failure. Tensile parameters were set according to ISO 527-1. The grip speed was set at 1 mm/min until the yield point was reached, and the rest of the test was carried out at a speed of 50 mm/min. The yield strength determination sensitivity was set at 0.1%. Four independent measurements were performed for each sample, and the results were an average of four.

Preparation and characterization of the feed water

In this study, the synthetic oil-in-brine emulsion was prepared by mixing crude oil with saline water. The oil-in-water emulsion was stabilized by polysorbate 20 (TWEEN 20) surfactant in an oil-surfactant ratio of 9:1 and ultrasonicated the mixture for 5 min. The resulting emulsion was kinetically stable and did not separate during the time of the experiment.

The composition of the crude oil was characterized by gas chromatograph (Agilent GS/MS). The temperature of both the detector and injector was 300 °C. For the initial isothermal period, the oven was heated at 60 °C for 3 min, then gradually heated at a rate of 20 °C/min up to 300 °C. The final isothermal period was 5 min, and the total run time was 20 min. Helium was used as the carrier gas at a flow rate of 0.233 ml/s. The processing of the resulting data was carried out using the MassHunter software.

Membrane testing system

Membranes' performance against oil-in-brine emulsion was tested using a pilot-scale AGMD system. A graphical representation of the system is given in Fig. 2.

1. Hot feed cycle.
2. Cooling fluid cycle.
3. The membrane unit
4. Monitoring and control.

The membrane unit consisted of a 400-cm² custom-made acrylic glass cell that was assembled by bolts and nuts, and the different cell compartments were isolated by rubber gaskets. The active flow area was 10 × 10 cm, and the flow channel depth was 2 mm in both the feed and cooling compartments. Two 45°-angled rhombus filament fiber spacers (single mesh size = 1.39 mm, filament diameter = 0.25 mm, and spacer thickness = 0.2 mm) were placed above and below the membrane to provide turbulence and to support the membrane, respectively. Galvanized steel was selected as the material of construction for the cooling plate due to its corrosion resistance and good thermal conductivity. The air-gap utilized was fixed at 9 mm and equipped with a permeate nozzle at the bottom.

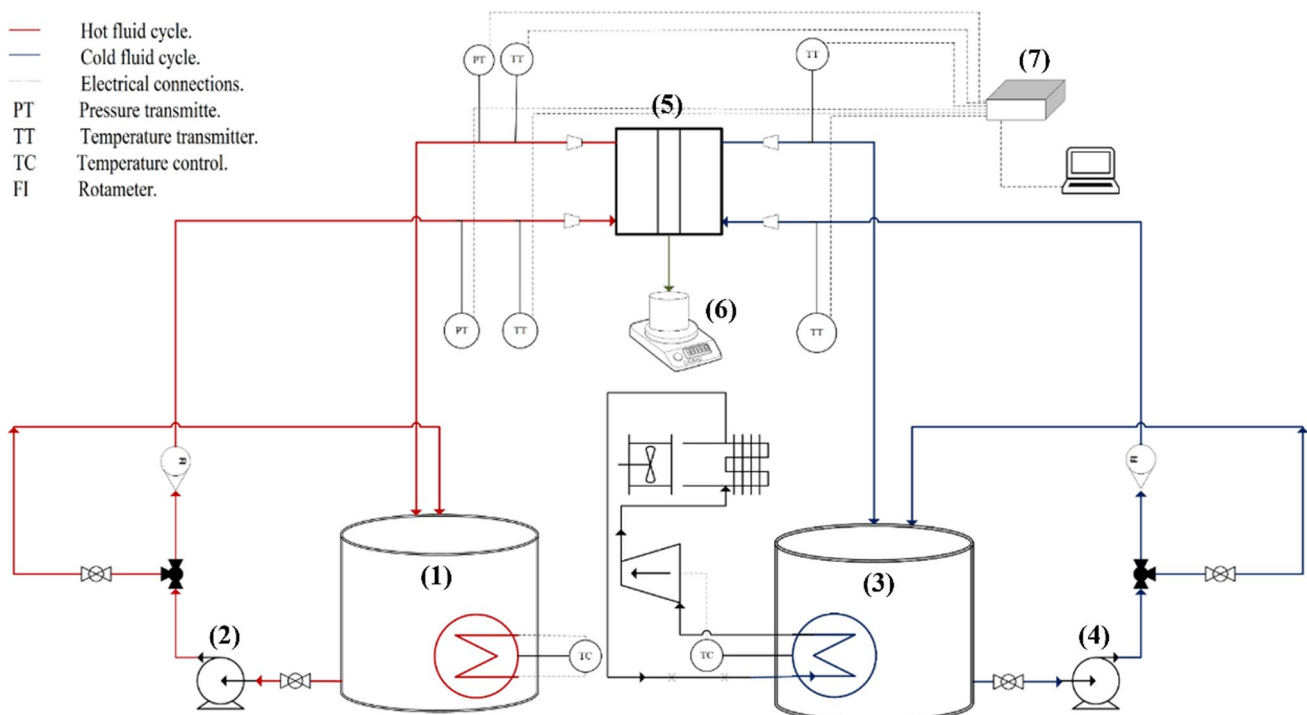


Fig. 2 Illustration of the pilot MD module utilized in this work: 1- polluted-water tank, 2- polluted-water pump, 3- cooling water tank, 4- cooling water pump, 5- membrane unit, 6- digital balance, and 7- data logger

Membrane performance evaluation

The separation efficiency of the membrane was tested in the AGMD system. The feed temperature considered in this work was 70 °C, and the cooling temperature was fixed at 20 °C. The feed flow rate was 2 l/min. The salinity was 40000 ppm, and the oil concentration was 200 ppm. A new membrane sheet was used in each experiment. Sampling of the permeate water was carried out every 30 min to measure the permeate water conductivity and check the occurrence of membrane wetting. The COD was measured once for every experiment using the dichromate method to account for the average amount of oil that escaped to the permeate. The tests were carried out for 10 h or until the removal efficiency reached 30%. The membrane was tested in continuous operation mode.

The permeate flux, J (l/m².h), is calculated using (Eq. 3):

$$J = \frac{W}{\rho A \Delta t} \quad (3)$$

where (W) is the permeate mass, (ρ) is the density of the permeate, (A) is the active cross-sectional area of the membrane, and (Δt) is the elapsed time.

Results and discussion

Crude oil characterization

The GC curve for the crude oil is shown in Fig. 3. GC results indicate that the crude oil is mostly straight chain and branched alkanes with a few aldehydes and cyclic aliphatic and aromatic hydrocarbons. These components readily foul the surface of the membrane due to the van der Waals attractions.

Membranes characterization

Surface morphology, elemental analysis, surface roughness, FTIR analyses, and mechanical stability results were collected and compared to investigate the behavior of fouling.

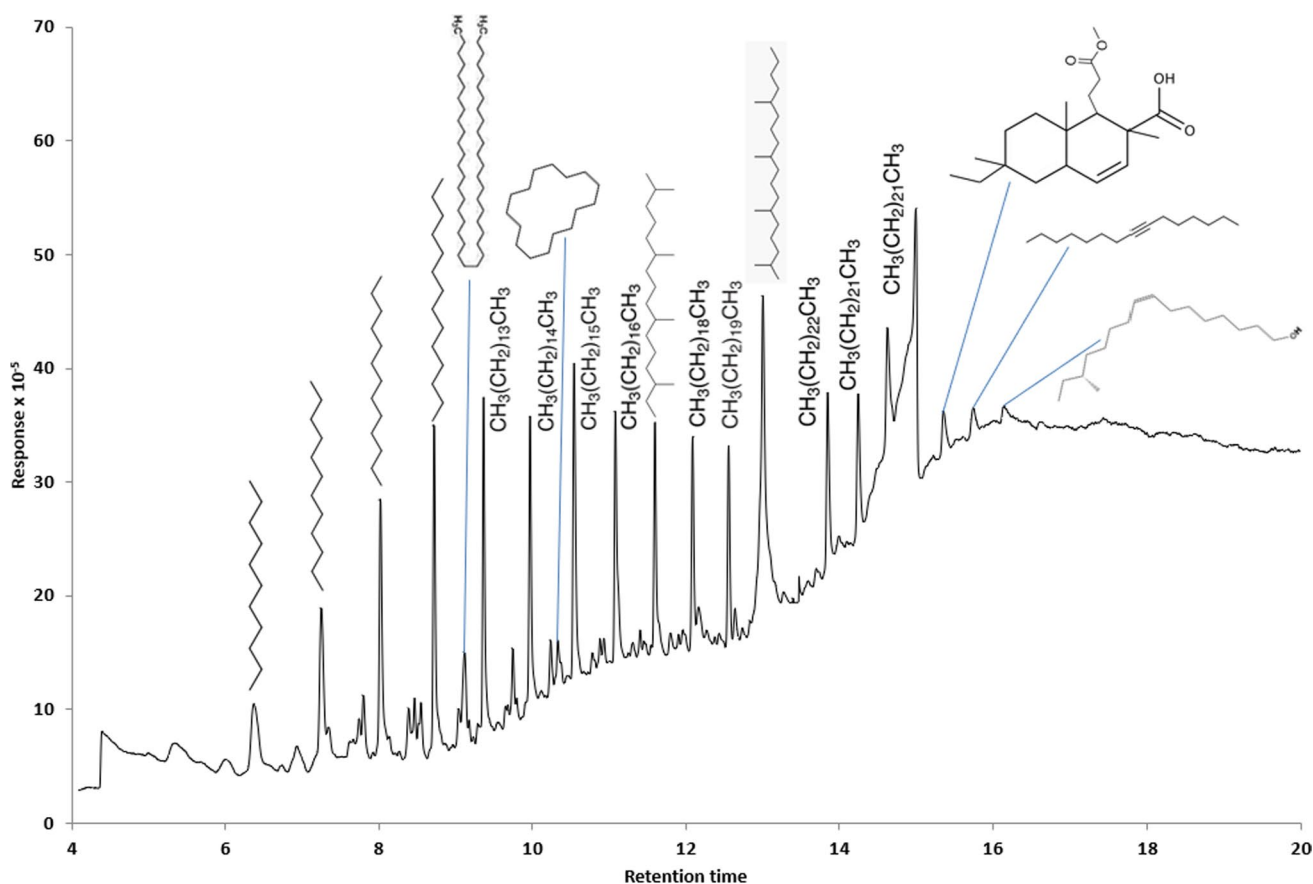


Fig. 3 Gas chromatography analysis of the crude oil utilized in this study (only the compounds with an area percentage greater than 1 are shown)

Surface morphology and surface composition

Scanning electron microscope (SEM) images of the pristine PTFE and modified PVDF membranes were captured at different magnifications. In MD operation, the surface hydrophobicity of the membrane is crucial to prevent the deposition of salts and membrane wetting. In addition to the presence of the hydrophobic C-F function group, the presence of a rough surface at the Cassie–Baxter state may capture micro air bubbles and minimize wetting. However, higher roughness may induce the deposition of inorganic scales. An overview SEM image of the PTFE membrane showing the support polypropylene layer is given in Fig. 4. The polypropylene support layer appears to be compressed onto the PTFE membrane. The SEM image in Fig. 4 shows that the support is highly porous with ellipsoidal openings equally distributed over the surface.

Figures 5 and 6 show the SEM images of the pristine PTFE membrane and the modified PVDF membrane,

respectively, at magnifications of 1, 2.5, 5, and 45 kx. The surface of the PTFE membrane is rough, irregular, and unsymmetric. The morphology resembles that of arrayed nanowires with a single wire diameter averaging between 50 and 250 nm. The morphology of the modified PVDF membrane resembles that of nanospheres arranged with nanometer roughness that is apparently less than that of the PTFE membrane.

Surface imaging was carried out after the treatment of oil-polluted water to assess the fouling behavior on the membranes' surfaces. Figure 7a shows the PTFE membrane sheet before and after oily-saline water treatment. The membrane surface became extremely fouled with oil after treatment, with the fouling intensity decreasing in the direction of flow. Figure 7b shows the SEM images of the membrane's top surface. The surface became almost completely covered with a multi-layer of foulants of variable morphology. The composition of the foulant layer reveals the nature of foulants and the tendency of each foulant to deposit on the surface.

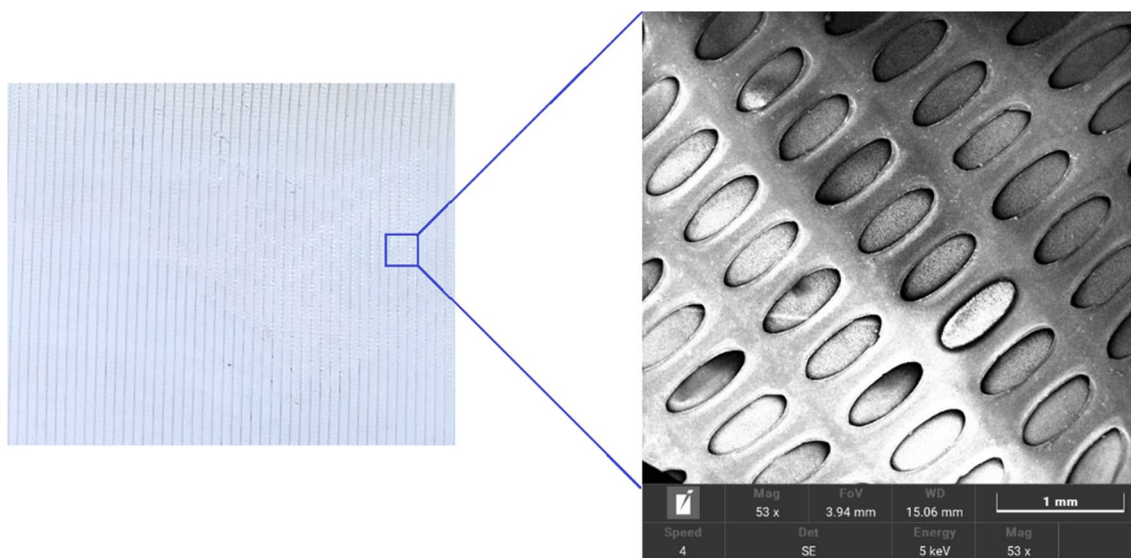


Fig. 4 Overview of the pristine PTFE membrane showing the support layer

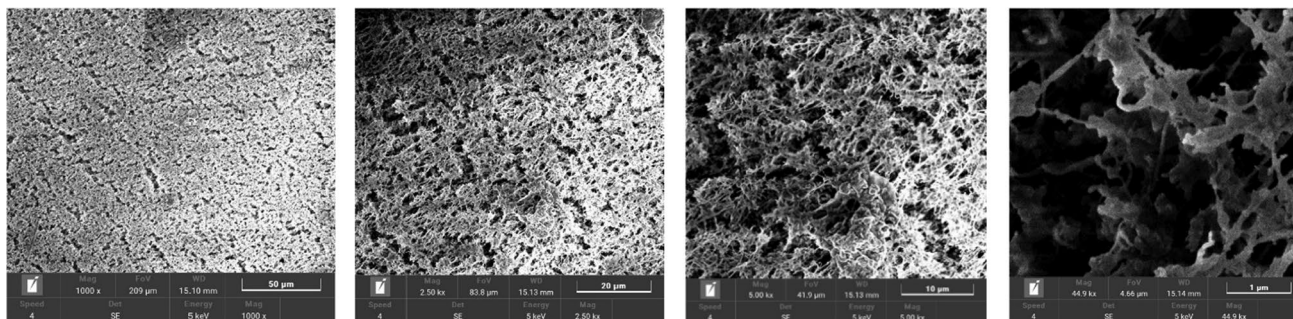


Fig. 5 Scanning electron microscope images of the pristine PTFE membrane

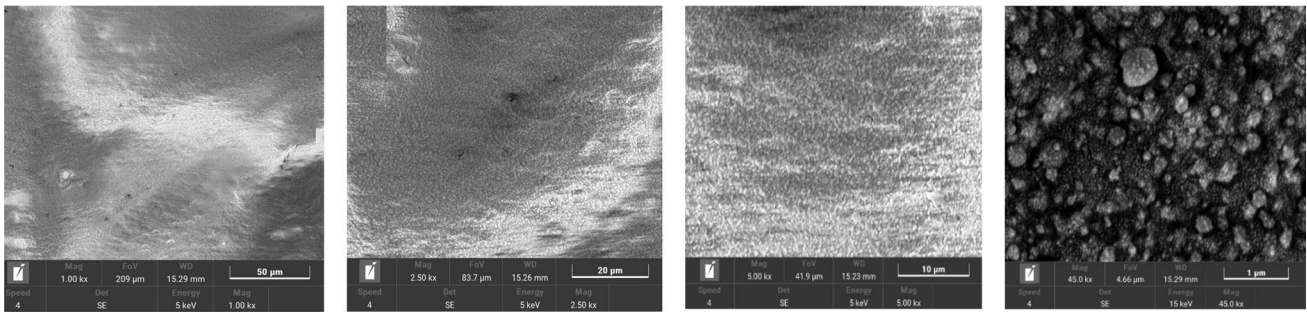


Fig. 6 Scanning electron microscope images of the modified PVDF membrane

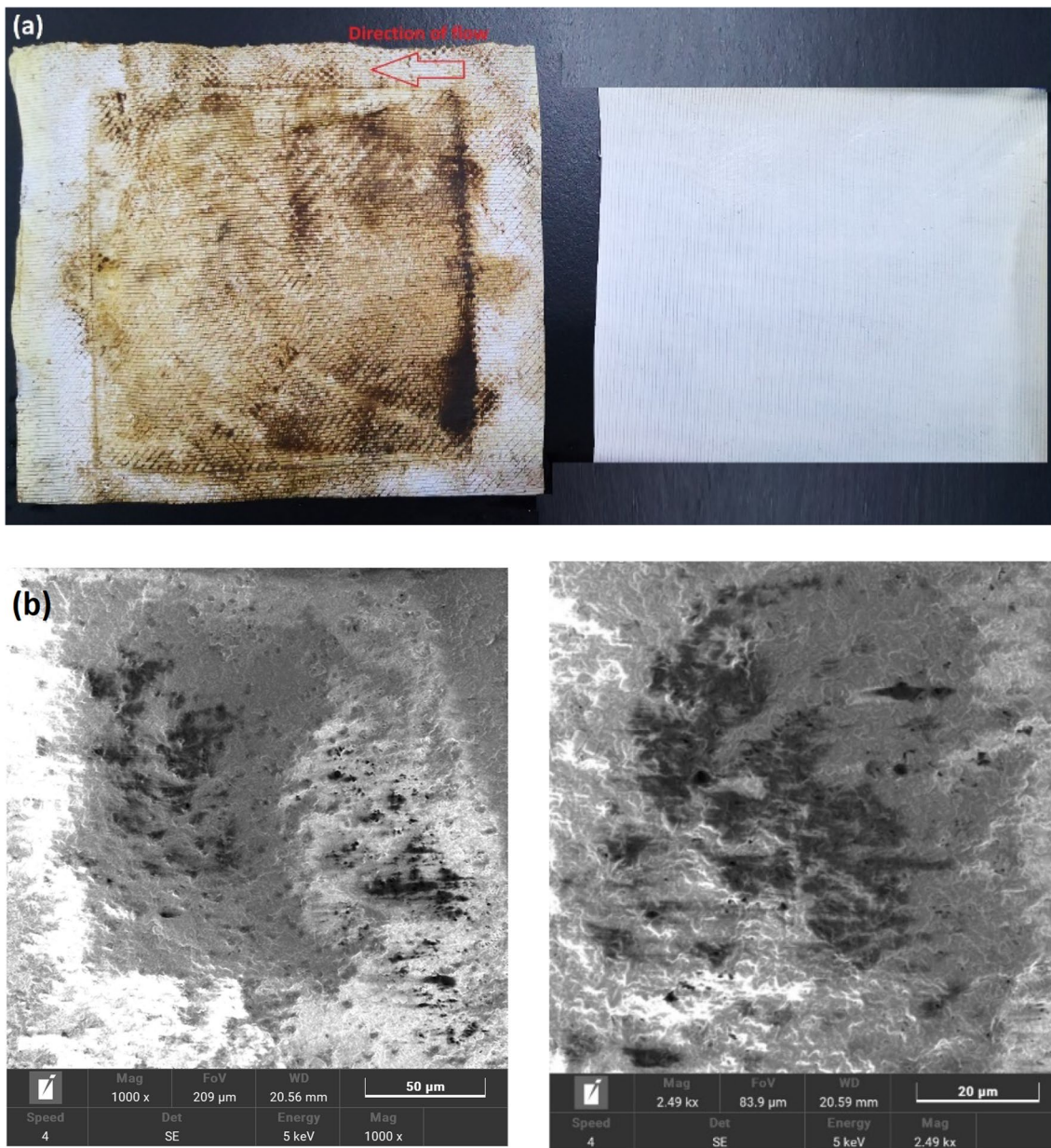


Fig. 7 Illustration of the fouling behavior on the PTFE membrane: **a** camera images and **b** SEM images

Elemental analysis by the EDS was performed on the membrane's top surface, and the results are presented in Fig. 8. It was observed that the large aggregates formed on the membrane surface were due to salt deposition. Some metals were detected on the membrane surface such as iron, copper, and zinc. The presence of metals in the feed solution should be attributed to the crude oil. Oxygen was detected throughout the membrane surface which could be attributed to both the metal oxides and the organic foulants from the crude oil. The increase in the concentration of carbon indicates the high concentration of organic foulants deposited. The extreme

fouling deposited on the membrane indicates the undeniable presence of membrane wetting. In order to assess the severity of wetting, imaging and elemental analysis of the membrane bottom was performed to check the diffusion of water across the membrane, and the results are shown in Fig. 9. The bottom of the membrane surface in the SEM image appeared to be not fouled, and the membrane pores were still obvious. However, the elemental mapping of the bottom surface revealed that some salts did diffuse and reached the bottom membrane surface. Sodium chloride diffused through the membrane in addition to iron, copper, and zinc.

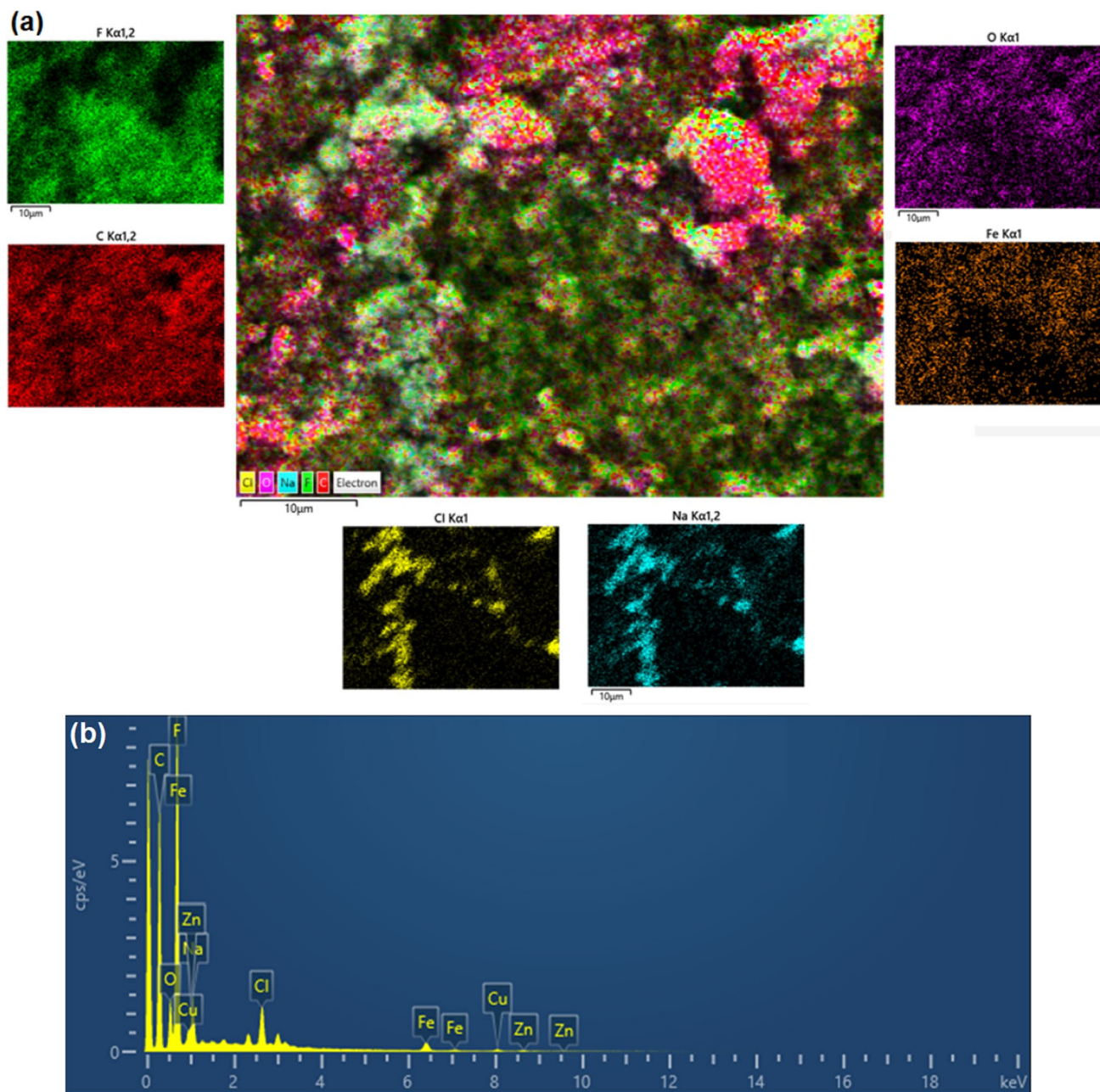


Fig. 8 EDS analysis of the fouled PTFE membrane surface: **a** elemental mapping with single-element distribution and **b** intensity chart

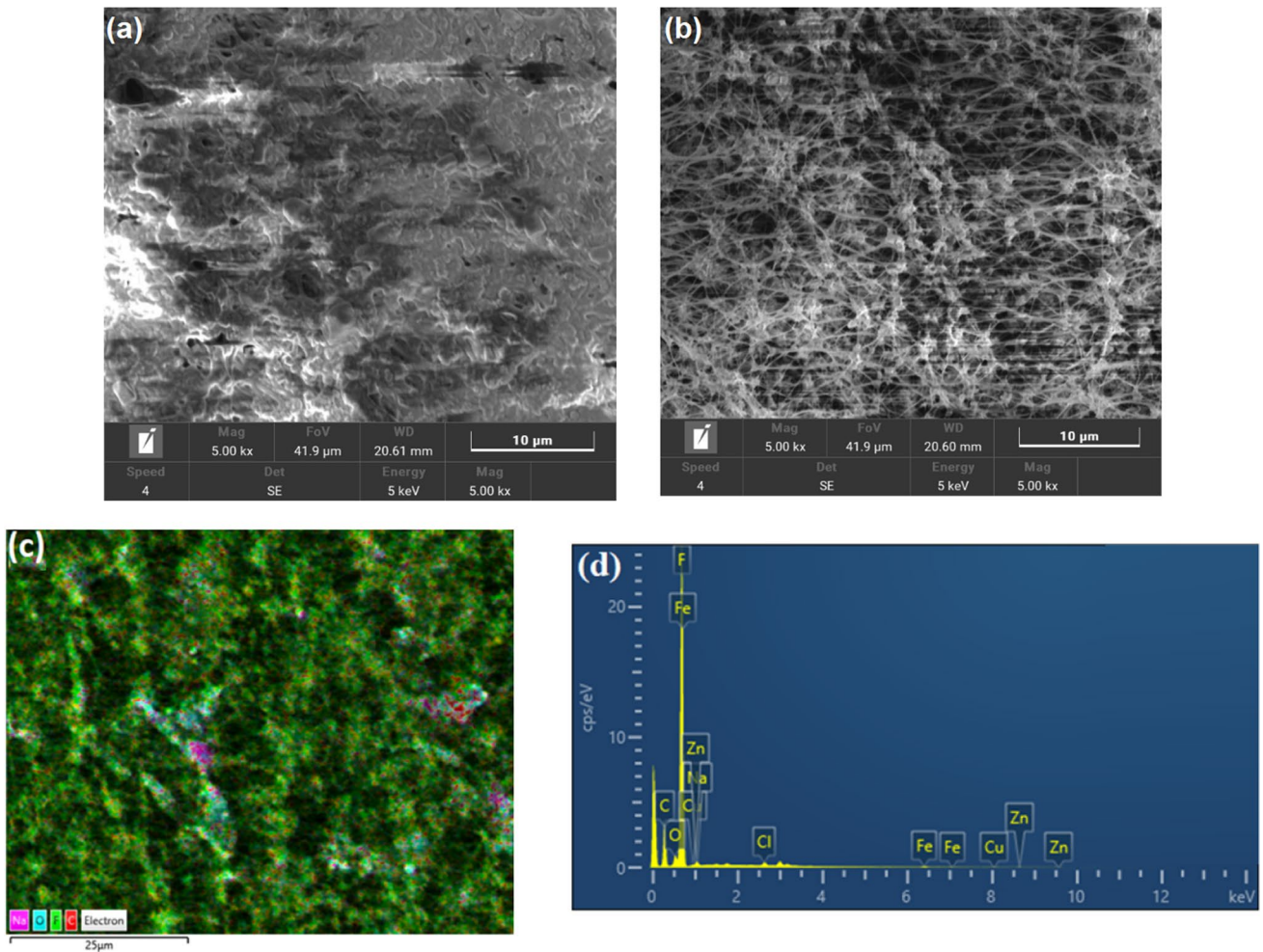


Fig. 9 **a** SEM image of the fouled membrane top surface, **b** SEM image of the PTFE membrane bottom surface, **c** elemental mapping of the bottom surface, and **d** intensity chart

The diffused salts did not accumulate considerably on the bottom of the surface; however, they indicate that membrane wetting occurred at some point. A comparison between the surface composition of the pristine PTFE membrane, fouled

membrane top surface, and fouled membrane bottom surface is given in Table 2. It can be deduced from the table that the composition of the membrane’s bottom surface did not vary

Table 2 EDS elemental analysis of the PTFE membrane before and after oily brine treatment

Element	Pristine PTFE membrane		PTFE membrane after treatment (Top)		PTFE membrane after treatment (Bottom)	
	Wt%	Atomic %	Wt%	Atomic %	Wt%	Atomic %
C	22.80	31.84	42.47	55.19	21.8	31.13
F	77.20	68.16	39.9	32.78	72.9	64.76
O	NA	NA	8.94	8.73	3	3.14
Na	NA	NA`	1.96	1.33	0.5	0.34
Cl	NA	NA	1.39	0.61	0.1	0.15
Fe	NA	NA	1.66	0.46	0.5	0.15
Cu	NA	NA	2.15	0.53	0.6	0.15
Zn	NA	NA	1.53	0.37	0.7	0.17
Total	100	100	100	100	100	100

much from the pristine membrane and that copper was the most abundant metal.

Figure 10a shows the PVDF membrane sheet modified with KOH before and after the pretreatment of oily brine. Oil fouling was much less severe than observed on the surface of the hydrophobic membranes. However, oil penetrated the membrane surface with water and deposited within the membrane pores and the support layer fibers which would increase the extent of irreversible fouling. Figure 10b shows the SEM images of the membrane's top surface. Fouling was in the form of flat scales equally distributed on the membrane surface. Elemental analysis was performed on the membrane's top surface to reveal the composition of the foulant layer, and the results are presented in Fig. 11. Higher concentrations of salts and metals were detected on the surface of the PVDF hydrophilic membrane after the treatment.

This is a common phenomenon in pressure-driven membrane processes since liquid water crosses the membrane surface, not water vapor as in the case of membrane distillation. Oil fouling was less severe due to the hydrophilic nature of the membrane surface. The presence of fluoride in the EDS spectrum was masked by the hydroxylated layer of the membrane surface. Imaging of the membrane bottom was performed to confirm the penetration of oil, and the results are shown in Fig. 12. The bottom of the membrane surface in the SEM image appeared to be severely fouled with scales and dense layers of foulants.

Figure 13a shows a visual observation of the pristine PTFE membrane and the PTFE membrane sheet after the treatment of the oily brine pretreated with ultrafiltration. No oil fouling was observed visually, and only minor mechanical deflection was observed. Figure 13b shows the SEM

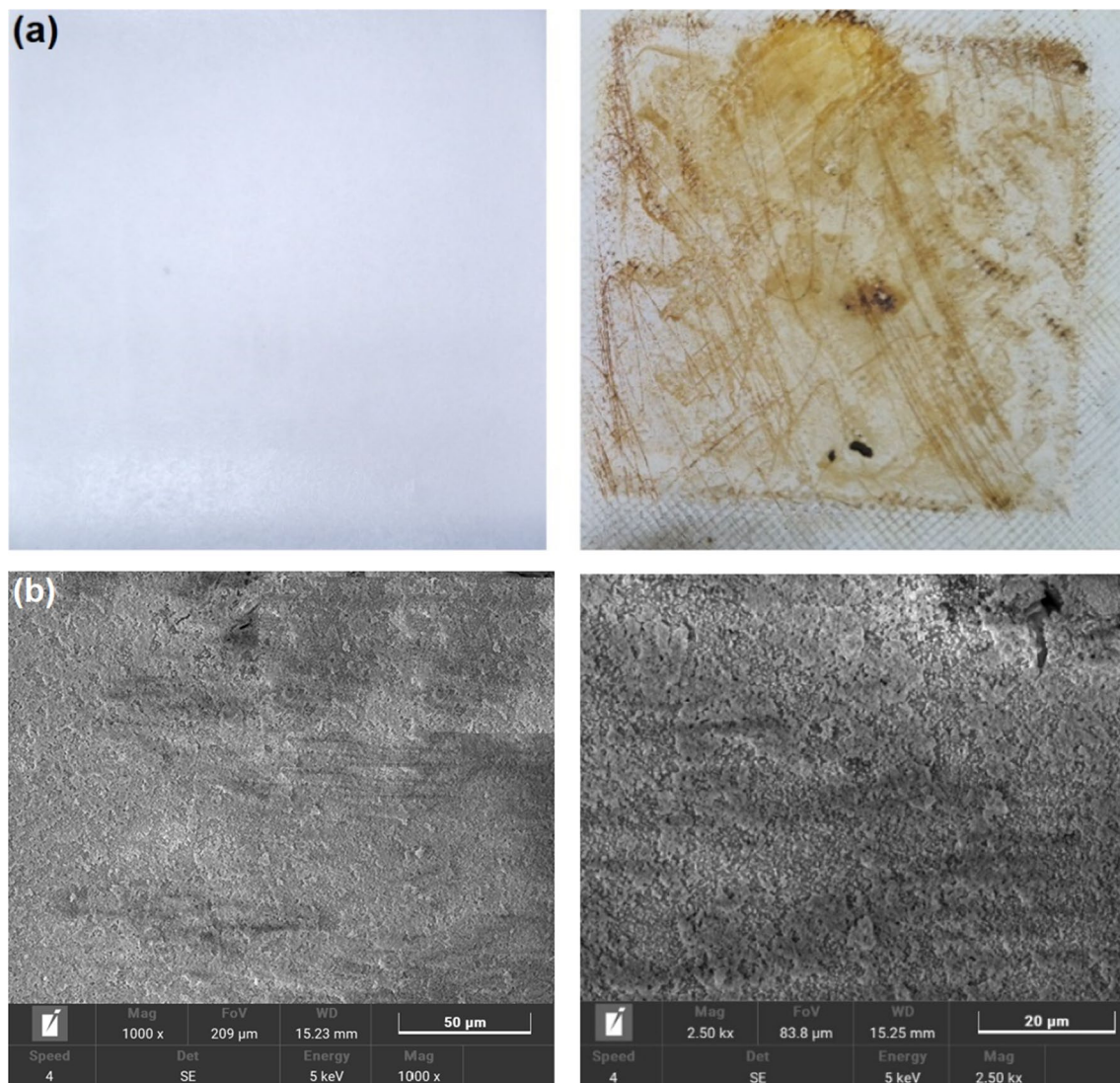


Fig. 10 Illustration of the fouling behavior on the modified PVDF membrane: **a** camera images and **b** SEM images

Fig. 11 EDS analysis of the fouled PVDF membrane surface: **a** elemental mapping and **b** intensity chart and elemental composition

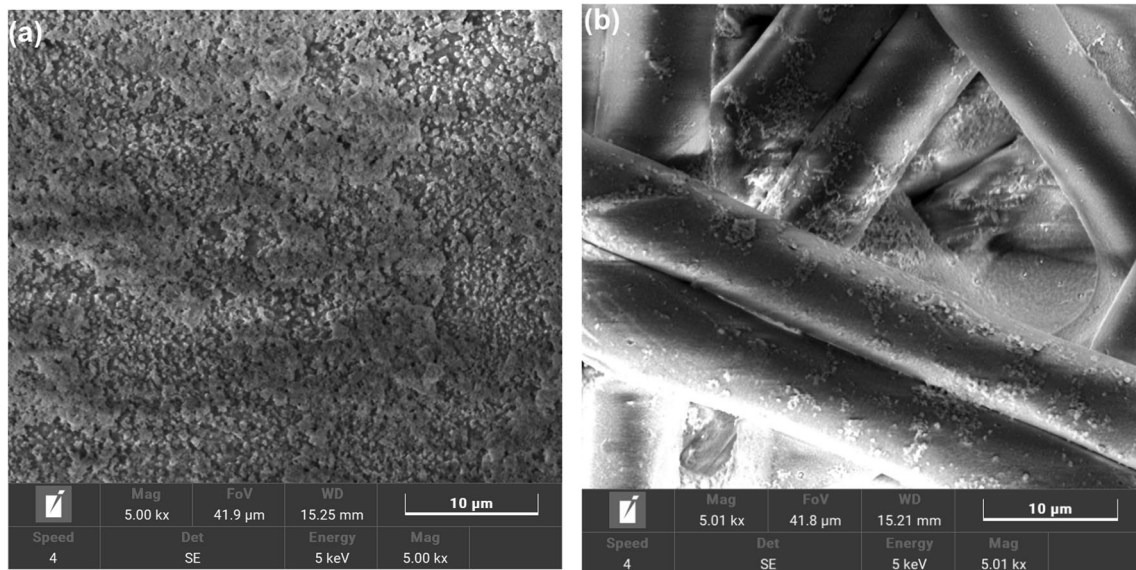
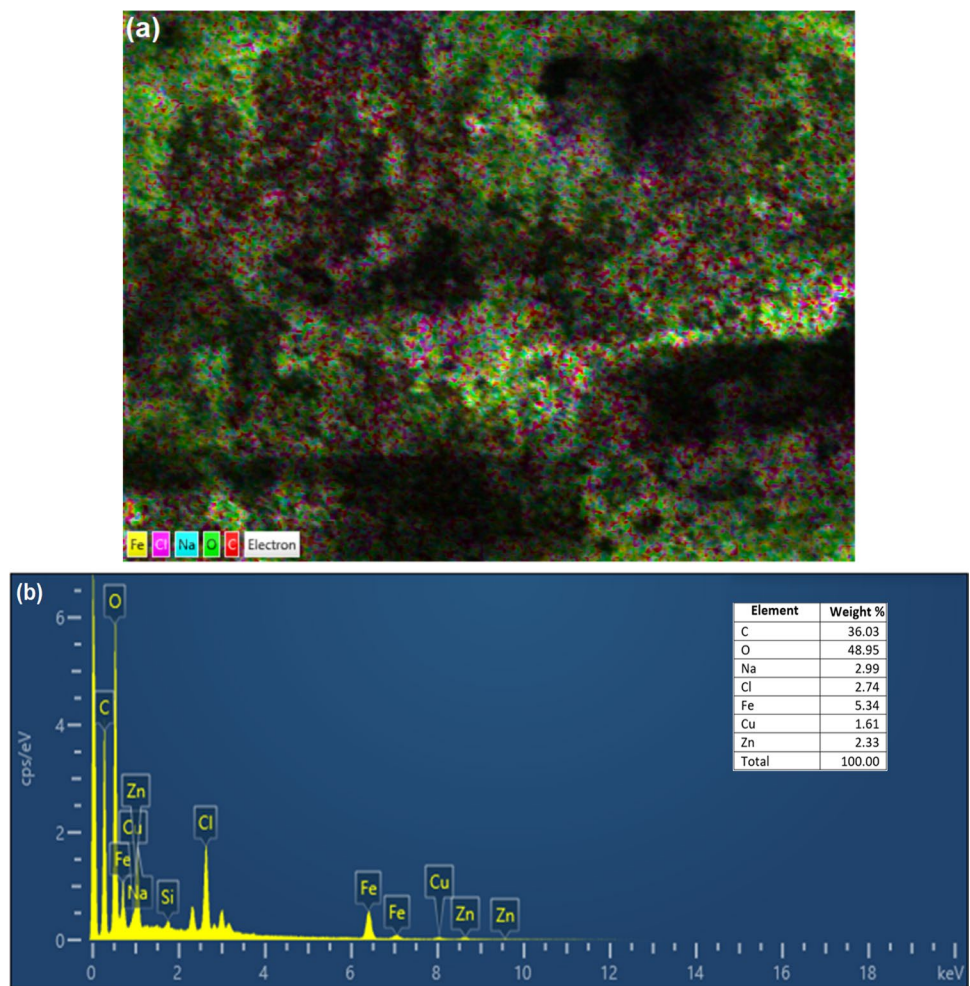


Fig. 12 **a** SEM image of the fouled PVDF+KOH membrane top surface and **b** SEM image of the fouled PVDF+KOH membrane bottom surface

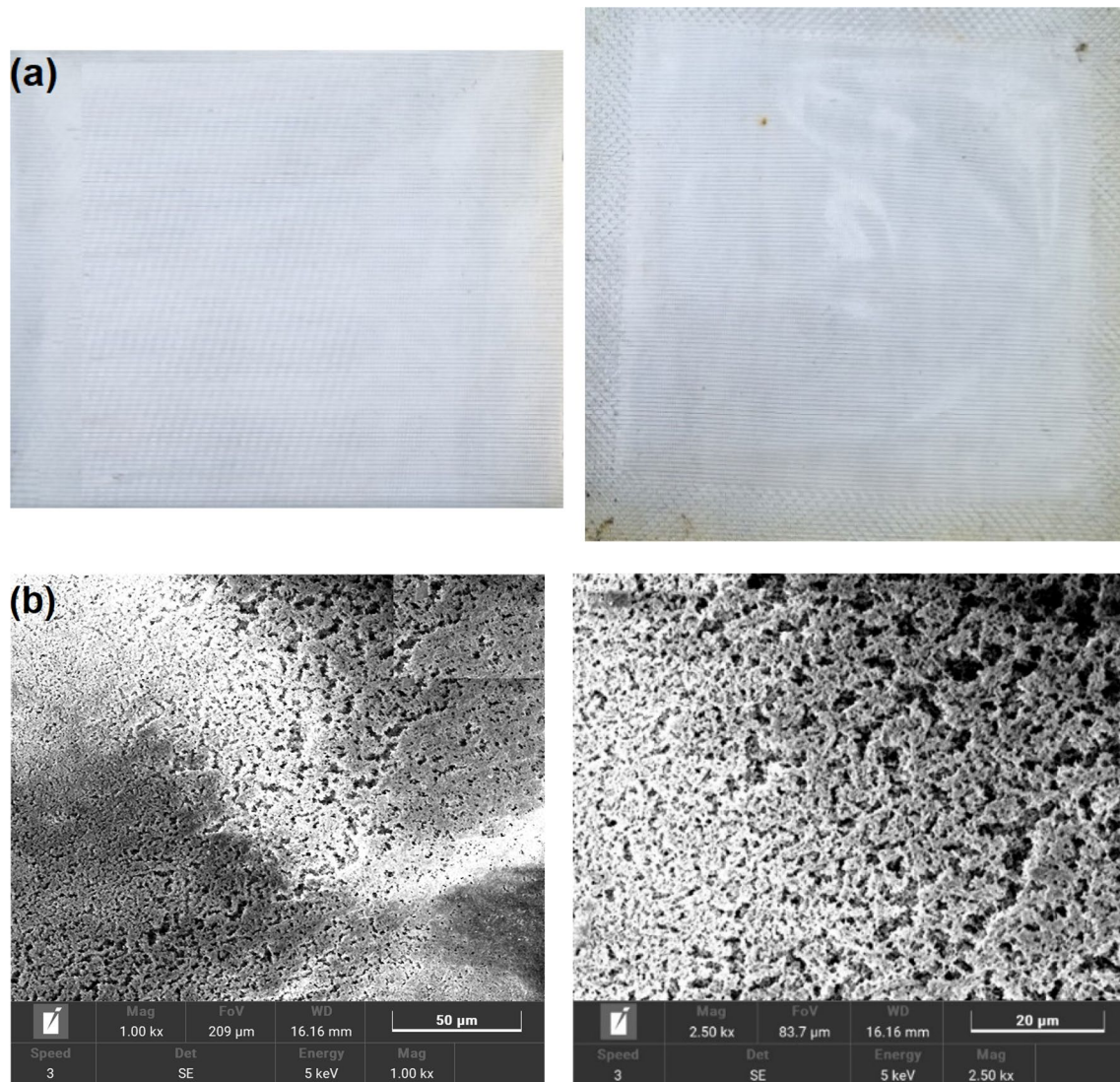


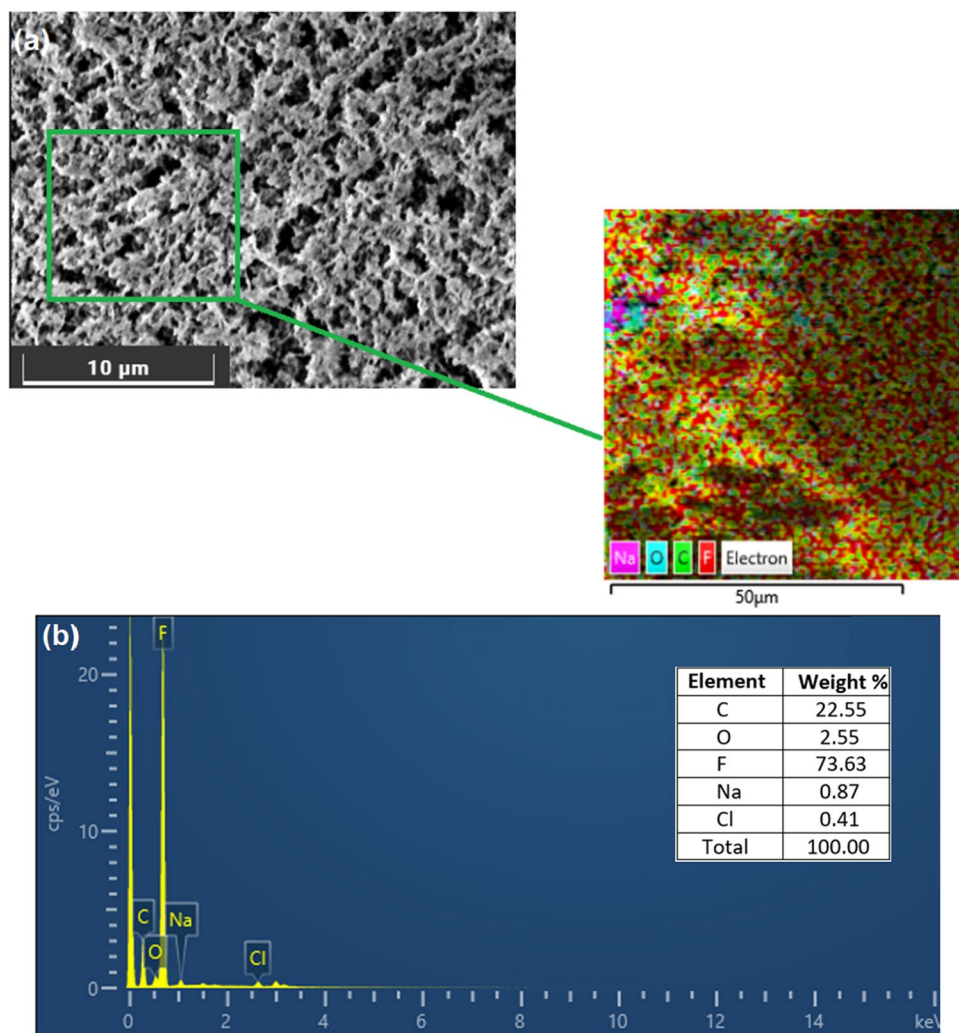
Fig. 13 Illustration of the fouling behavior on the PTFE after the treatment of the oily brine pretreated with ultrafiltration: **a** camera images and **b** SEM images

images of the membrane's top surface. The surface became slightly covered with a foulant layer. Elemental analysis was performed on the membrane's top surface to identify the foulants, and the results are presented in Fig. 14. Results showed the significance of pretreatment prior to the membrane distillation process. Only sodium salts were observed on the membrane surface, and the metals were eliminated in the pretreatment process. The presence of oxygen implied the presence of organic foulants. Oil fouling was not observed visually because most of the suspended and emulsified oil were eliminated in the pretreatment step. However, dissolved components of the crude oil in water were deposited onto the membrane surface.

Membrane backwashing with water is a common process in industry utilized to remove the deposited foulants.

Therefore, water washing of the fouled PTFE membrane was carried out to assess its effectiveness in eliminating the deposited foulants. Figure 15 shows the SEM images of the PTFE membrane after backwashing with a constant stream of 3 L/min distilled water for 10 min. Water washing partially restored the initial condition of the PTFE surface. The surface morphology of the PTFE membrane reappeared after washing, and the foulants remaining were those attached to the polymer fibers. Elemental analysis was performed to determine the fouling layer behavior after water washing, and the results are given in Fig. 16. The elemental analysis revealed that inorganic salts were completely removed from the surface of both membranes. Copper and zinc were eliminated from the PTFE membrane surface, and the iron concentration was minimized. Organic foulants elimination

Fig. 14 EDS analysis of the fouled PTFE membrane surface: **a** elemental mapping and **b** intensity chart and elemental composition



was not considerable with water since organics tend to attach to the polymeric membrane surface and are less water soluble than salts.

Surface roughness

Atomic force microscopy analysis is a highly reliable technique to examine the nano-scale membrane architecture. Figure 17 shows the 2D color height images and the respective 3D height images of the PTFE membrane. The AFM results confirmed the observations of the scanning electron microscopy images that the surface roughness of the PTFE membrane was higher than that of the PVDF membrane. As shown in Fig. 17, large broad peaks were detected on the surface of the PTFE membrane which was consistent with the SEM images. These broad peaks are attributed to the crosslinking of the polymer structures (Bajpai et al. 2016). The presence of such peaks may act as a reentrant structure and capture micro air bubbles that reduce fouling deposition. The average line roughness parameter R_a and area roughness

parameter S_a of the PTFE membrane were 0.7 and 0.73 μm , respectively.

Fourier transform infrared spectroscopy

Fourier transform infrared spectroscopy analysis was performed on the membrane samples after oily brine treatment. Figure 18 shows the FTIR absorbance spectrum of the PTFE membrane before and after oily brine treatment. The characteristic peaks of the PTFE membrane at 1205 cm^{-1} , 1149 cm^{-1} , and 630 cm^{-1} remained unchanged indicating that organic foulants only deposited physically onto the membrane surface (i.e., no chemical bond formation). New peaks were observed at 1372 cm^{-1} , 1453 cm^{-1} , and 3316 cm^{-1} indicating the presence of O–H functional group of carboxylic acids and alcohols. The change in the behavior of the peak at 755 cm^{-1} and at the higher wavenumber range $2875\text{--}2950\text{ cm}^{-1}$ indicate the presence of different alkanes deposited from the crude oil. Figure 19 shows the FTIR absorbance spectrum of

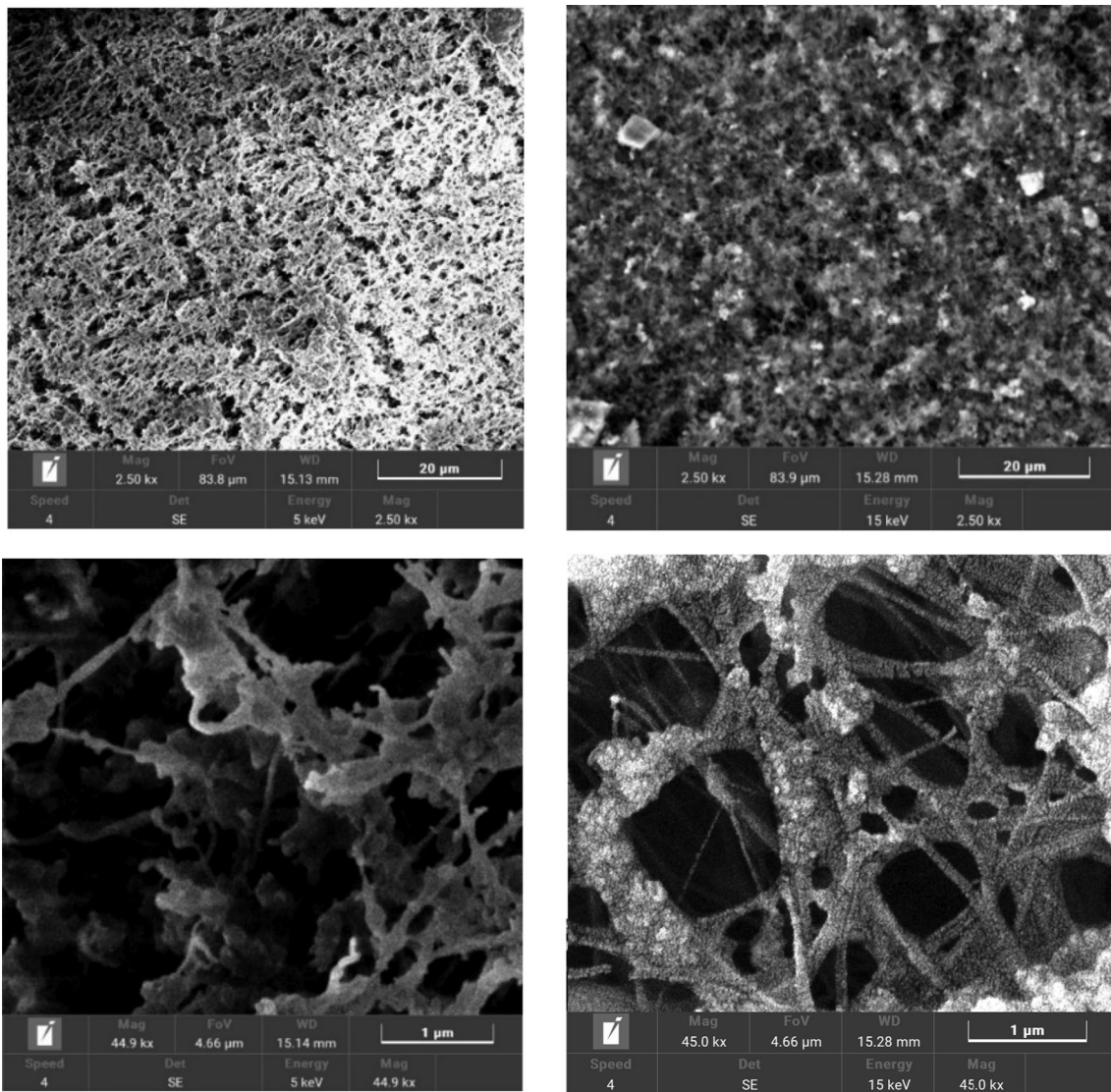


Fig. 15 SEM images of (left) pristine PTFE membrane (right) fouled PTFE membrane after washing with water

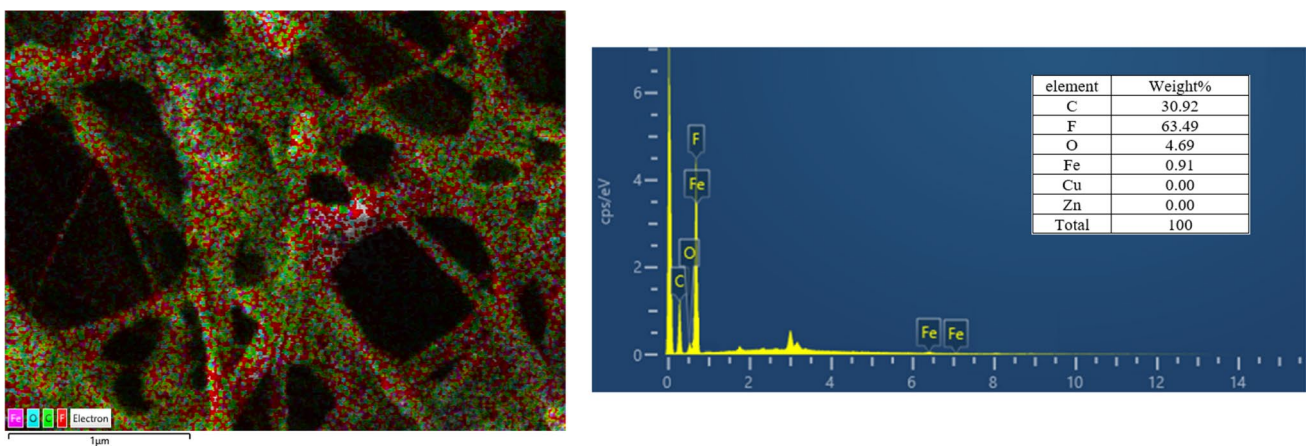


Fig. 16 Elemental mapping of (left) PTFE membrane after water washing and (right) PVDF membrane after water washing

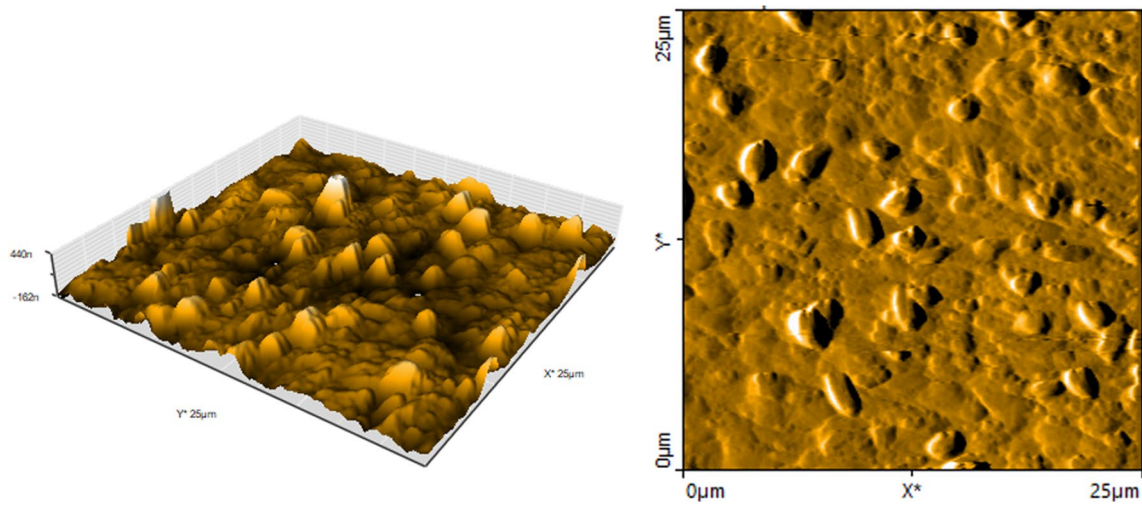
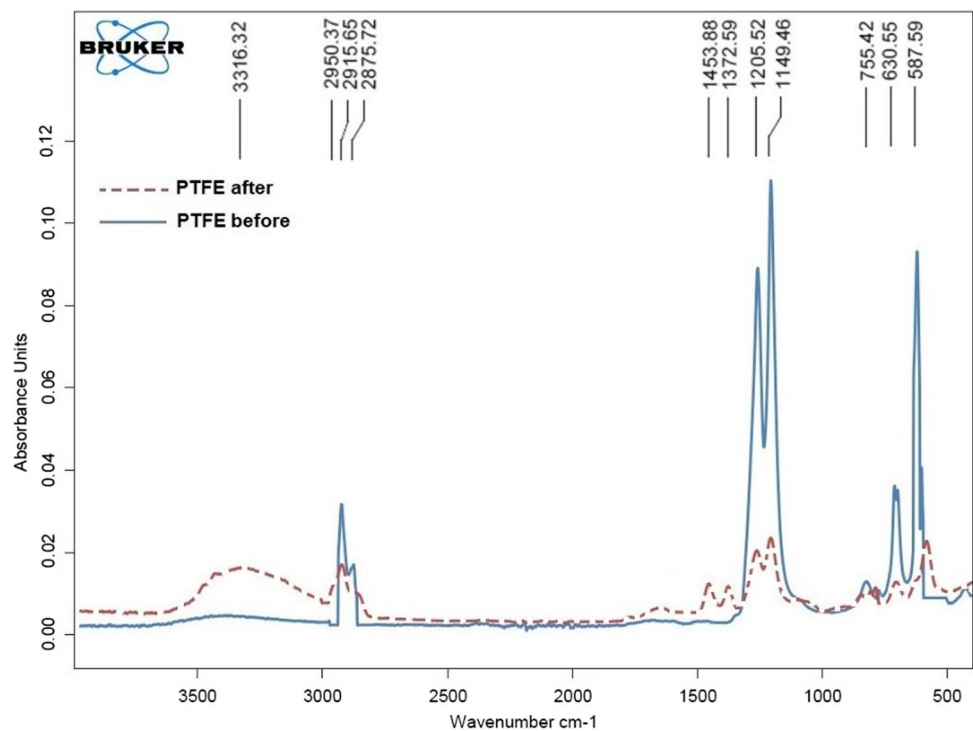


Fig. 17 2D color height images and 3D height images of the PTFE membrane

Fig. 18 FTIR absorbance spectrum of PTFE membrane before and after oily brine treatment



the PVDF + KOH membrane before and after oily brine treatment. Peaks shifting was not observed indicating the absence of chemical bonds between the crude oil and the membrane. This can be explained by the hydrophilic surface of the PVDF + KOH membrane. The characteristic peaks of the PVDF membrane appear at 840 and 1090 cm^{-1} , while the characteristic peaks of the polyester support layer appear at 1020 cm^{-1} , 1240 cm^{-1} , and 1712 cm^{-1} . The (O–H stretching of alcohol group) broad

peak from 3000 to 3500 cm^{-1} and the (O–H stretching of carboxyl group) broad peak at 2900 cm^{-1} indicate the successful substitution reaction between the hydroxyl and fluoride ions (Bhattacharya and Chaudhari 2014; Daems et al. 2018). The peaks at 2855 and 2918 cm^{-1} represent the C–H stretching of crude oil alkanes.

Fig. 19 FTIR absorbance spectrum of PVDF + KOH membrane before and after oily brine treatment

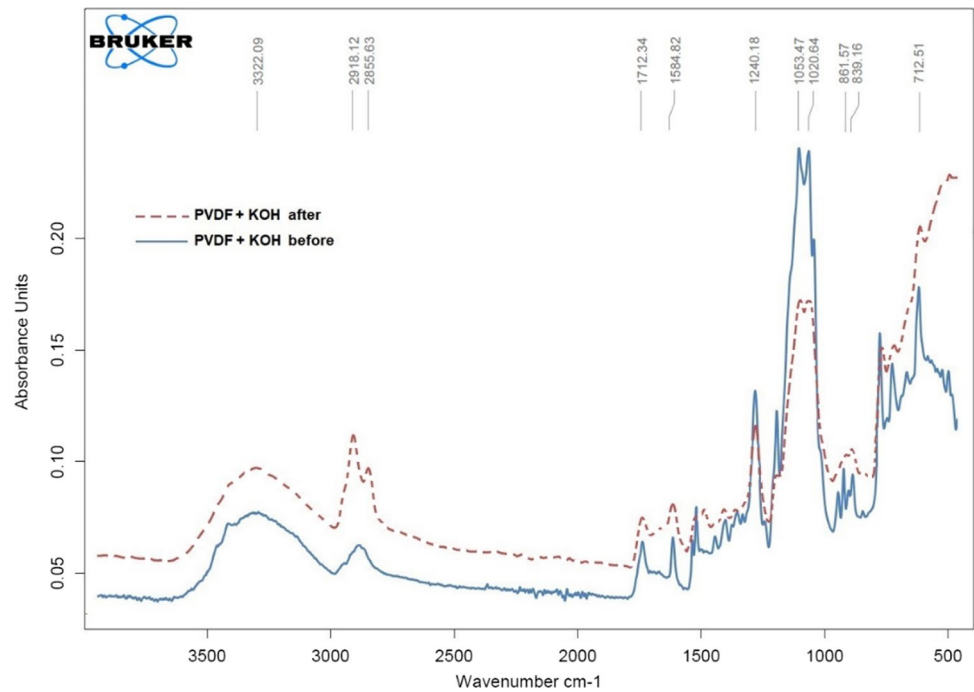
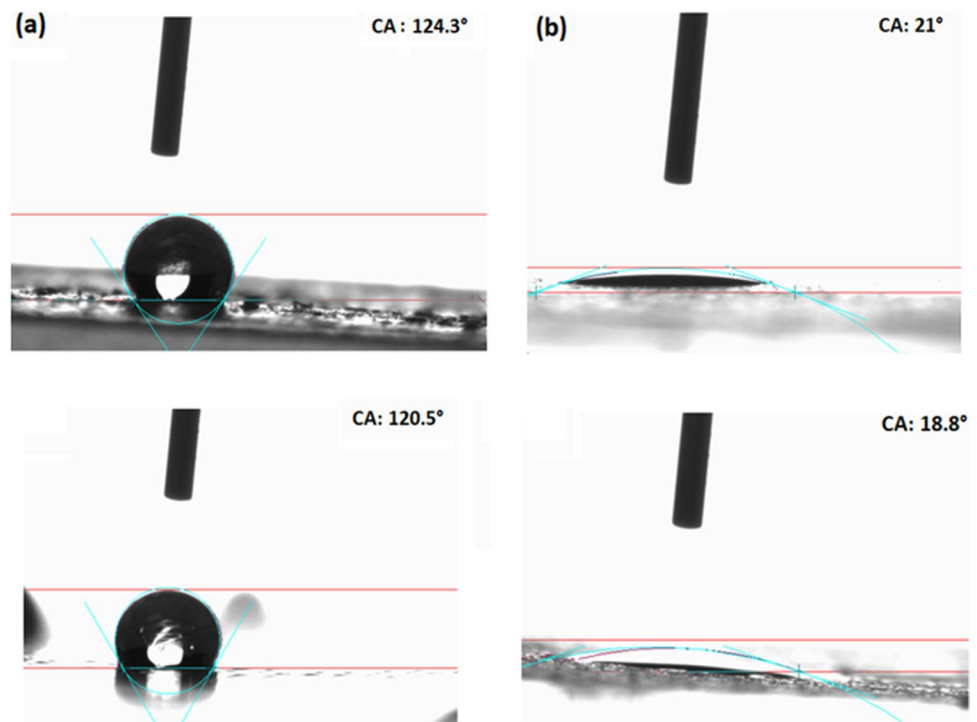


Fig. 20 Water contact angle of **a** PTFE membrane and **b** modified PVDF membrane before (top) and after (bottom) oily brine treatment



Surface wettability

Water contact angle measurements were conducted after oily brine treatment to observe the variation in the surface tension of the PTFE and the PVDF membranes. Figure 20 shows the measured contact angles of the two membranes.

The average water contact angle of the PTFE membrane reduced slightly from 124.3° to 120.5°. The hydrophilic PVDF membrane experienced a mild reduction in the water contact angle from 21° to 18.8°. The reduction in the water contact angle either for the hydrophobic or the hydrophilic membranes was due to the salt deposition onto the

membranes' surfaces. Salts, being polar compounds, reduce the surface tension between the membrane and water molecules (Goodarzi and Zendehboudi 2019).

Mechanical stability

Tensile tests were carried out to assess the mechanical stability of the membranes before and after the treatment of the oily brine. Figure 21 summarizes the results of the tensile tests. The PVDF membrane had a higher mechanical strength than the PTFE membrane. This can be attributed to the inherent high mechanical strength of the polyester support layer. After the treatment of the oily brine, the modified PVDF membrane exhibited a considerable reduction in its mechanical stability. The maximum stress of the membrane could withstand before breaking was reduced by 15%. This is attributed to the oily brine penetrating the membrane causing mechanical and possibly chemical deformation.

The PTFE membrane, in spite of its lower mechanical strength, sustained its mechanical stability after the treatment of produced water. The hydrophobic and rough nature of the PTFE membrane hindered the penetration of liquid molecules consequently minimizing wetting and irreversible fouling.

Membrane performance in the AGMD tests

Figure 22 shows the results of oily brine treatment by standalone AGMD using the PTFE membrane. The performance curve trend approaches that of a sinusoidal wave. Initially, the flux was 6 L/m².h, and the salt rejection was 99.1%. The flux deteriorated slowly over 60 min to 5.15 L/m².h and the rejection to 98%. At the time interval of 60–150 min, the rejection deteriorated rapidly to 52.63%, and the flux increased correspondingly to 13.7 L/m².h. At the time interval of 150–270 min, the rejection increased rapidly to 94.1%,

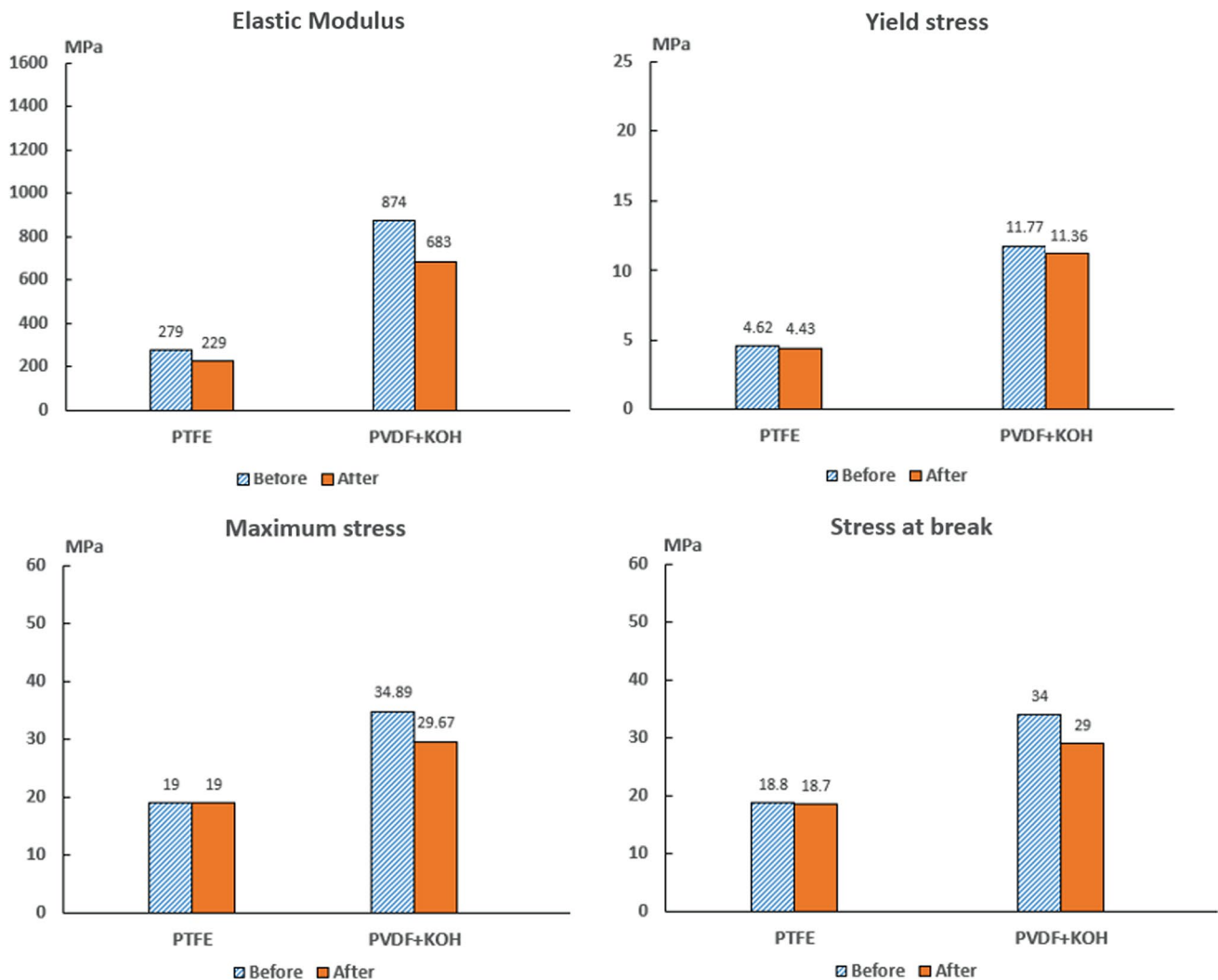
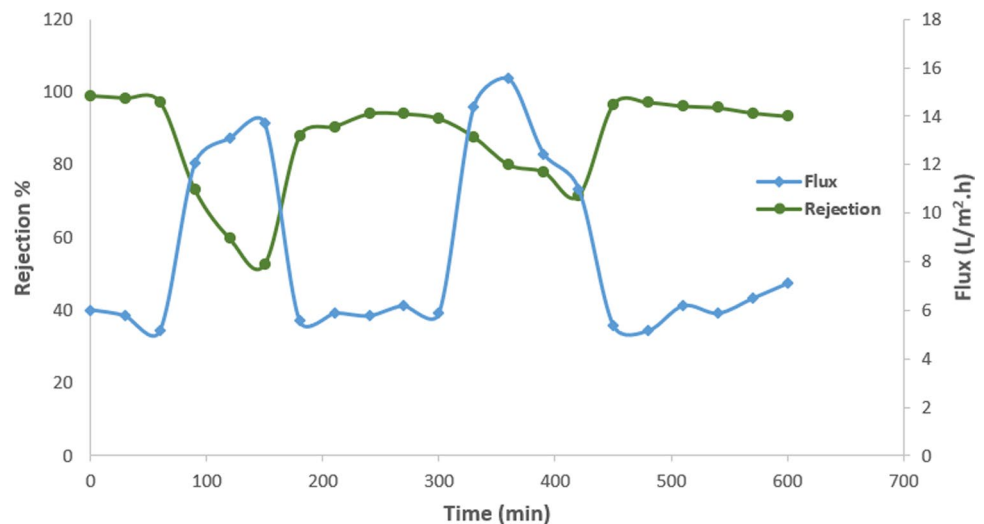


Fig. 21 Mechanical properties of the PTFE membrane, PVDF membrane, and PVDF + KOH membranes before and after PW treatment

Fig. 22 Membrane performance testing for experiment 1 (PTFE membrane, 70 °C, 2 L/min)



and the flux regained its initial range at 6.1 L/m².h. The trend was repeated at the time intervals of 270–420 min and 420–600 min, respectively. However, the deterioration in rejection was less severe and stabilized at the end of the 10-h run at 93.5%. The first sinusoidal wave was most likely attributed to the interchanging deposition and erosion of foulants. Initially, flux declined due to initial pore blocking. The deposition of a secondary layer of salts and oil caused gradual membrane wetting which decreased the mass transfer resistance and facilitated the passage of salts. The particle size of the foulants continued to grow until it was possible to be removed by the feed flow momentum which restored the initial condition of the membrane rapidly. The behavior reoccurrence with less severity is attributed to the presence of a stable foulants layer that blocked the pores. Pore blocking minimized the passage of salts consequently increasing the rejection. The average oil rejection was 95.1%.

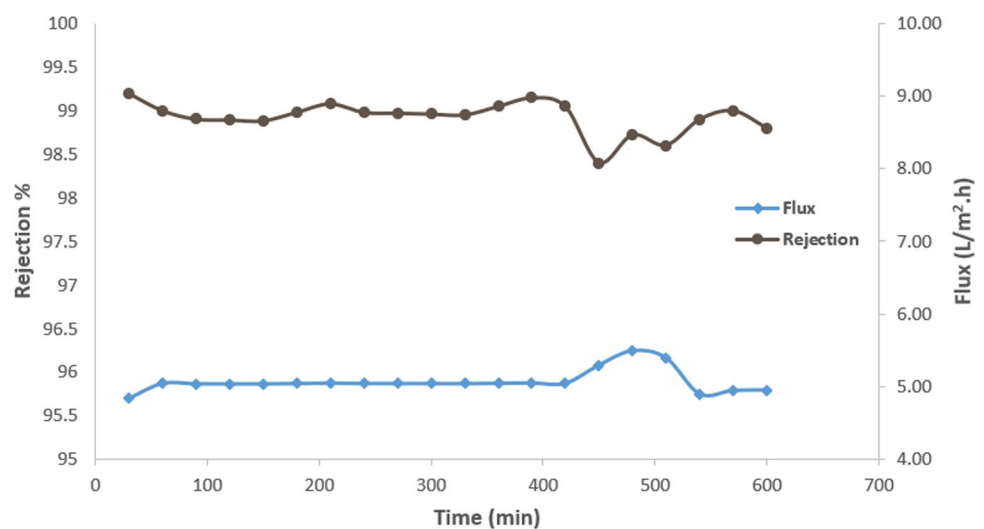
Feed pretreatment by ultrafiltration using the modified PVDF membrane was tested with the PTFE membrane to

enhance the process stability. Figure 23 shows the results of the hybrid system. The rejection and flux were stable throughout the experiment time with only mild fluctuations. The average flux was 5.07 L/m².h, and the salt rejection was always higher than 98.5%. The average oil rejection was 96.5%.

Conclusion

The treatment of produced water by standalone membrane distillation is not a sustainable approach. Severe wetting and fouling were observed on the surfaces of the tested hydrophobic membranes. The incorporation of an ultrafiltration pretreatment step greatly enhanced the process stability. The hybrid system comprising ultrafiltration pretreatment using the PVDF + KOH membrane followed by AGMD using the PTFE membrane exhibited the best operational stability and achieved the highest rejection of

Fig. 23 Membrane performance testing for experiment 2 (PTFE membrane after ultrafiltration pretreatment, 70 °C, 2 L/min)



both salt and oil. The salt rejection by the superior hybrid system was higher than 98.5%, and the oil rejection was 96%. This work intensively investigated the fouling and wetting phenomena on the polytetrafluoroethylene membrane and polyvinylidene fluoride membrane modified with KOH. Oil fouling on the modified PVDF membrane was much less severe than that observed on the surface of the hydrophobic PTFE membrane. However, oil penetrated the membrane surface with water and deposited within the membrane pores and the support layer fibers which increased the extent of irreversible fouling and deteriorated its mechanical stability. In the standalone AGMD experiments using the PTFE membrane, fouling was in the form of large aggregates composed of oil, salts, and metals. The severe membrane wetting resulted in salt and metals passage which were detected by the increase in the permeate conductivity and by the elemental analysis of the membrane bottom. A significant reduction in fouling was observed after ultrafiltration incorporation. Only sodium salts were observed on the membrane surface, and the metals were removed in the pretreatment process. The detection of oxygen in the elemental analysis implied the presence of organic foulants. Dispersed components of the crude oil in water escaped the ultrafiltration membrane and should be minimized by other processes such as stripping or chemical oxidation. The gas chromatography of the crude oil and FTIR analysis of the fouling layers showed analogous results. The organic fouling layer contained of aliphatic hydrocarbons and some hydroxyl-containing compounds. No peak shifting was observed in the FTIR analysis of the PTFE and modified PVDF membranes after fouling which indicated that the organic fouling layer did not attach chemically to the membranes' surfaces. The PTFE membrane sustained its hydrophobicity and mechanical stability to a greater extent after oil fouling.

Authors' contributions This study was conceptualized and designed by AEM, SMEM, YE, and MB with information and data collection conducted by a team including AEM, YE. The manuscript was written by AEM and MB. The manuscript was revised and approved by SMEM and MB. The authors read and approved the final manuscript.

Funding Open access funding provided by The Science, Technology & Innovation Funding Authority (STDF) in cooperation with The Egyptian Knowledge Bank (EKB).

Data availability Upon reasonable request, the corresponding author can provide access to the datasets generated during the study.

Declarations

Conflict of interest The authors declare no competing interests.

Open Access This article is licensed under a Creative Commons Attribution 4.0 International License, which permits use, sharing, adaptation, distribution and reproduction in any medium or format,

as long as you give appropriate credit to the original author(s) and the source, provide a link to the Creative Commons licence, and indicate if changes were made. The images or other third party material in this article are included in the article's Creative Commons licence, unless indicated otherwise in a credit line to the material. If material is not included in the article's Creative Commons licence and your intended use is not permitted by statutory regulation or exceeds the permitted use, you will need to obtain permission directly from the copyright holder. To view a copy of this licence, visit <http://creativecommons.org/licenses/by/4.0/>.

References

- Adetunji AI, Olaniran AO (2021) Treatment of industrial oily wastewater by advanced technologies: a review. *Appl Water Sci* 11(6):98
- Ahmad NA, Goh PS, Yogarathinam LT, Zulhairun AK, Ismail AF (2020) Current advances in membrane technologies for produced water desalination. *Desalination* 493:114643
- Bajpai AK, Bhatt R, Katare R (2016) Atomic force microscopy enabled roughness analysis of nanostructured poly (diaminonaphthalene) doped poly (vinyl alcohol) conducting polymer thin films. *Micron* 90:12–17
- Bhattacharya SS, Chaudhari SB (2014) Study on structural, mechanical and functional properties of polyester silica nanocomposite fabric. *Int J Pure Appl Sci Technol* 21(1):43
- Cai Y, Qin Z (2022) Review and Medium-and Long-Term Prospect of Global Oil Demand. In: Annual report on China's petroleum, gas and new energy industry (2021). Springer, pp 115–128
- Daems N, Milis S, Verbeke R, Szymczyk A, Pescarmona PP (2018) Vankelecom IFJ high-performance membranes with full pH-stability. *RSC Adv* 8:8813–8827
- Deka BJ, Guo J, Khanzada NK, An AK (2019) Omniphobic re-entrant PVDF membrane with ZnO nanoparticles composite for desalination of low surface tension oily seawater. *Water Res* 165:114982
- Devatha CP, Vishnu Vishal A, Purna Chandra Rao J (2019) Investigation of physical and chemical characteristics on soil due to crude oil contamination and its remediation. *Appl Water Sci* 9:1–10
- Elhady S, Bassyouni M, Mansour RA, Elzahar MH, Abdel-Hamid S, Elhenawy Y, Saleh MY (2020) Oily wastewater treatment using polyamide thin film composite membrane technology. *Membranes (basel)* 10(5):84
- Elhenawy Y, Moustafa GH, Abdel-Hamid SMS, Bassyouni M, Elsakka MM (2022a) Experimental investigation of two novel arrangements of air gap membrane distillation module with heat recovery. *Energy Rep* 8:8563–8573
- Elhenawy Y, Moustafa GH, Attia AM, Mansi AE, Majozi T, Bassyouni M (2022) Performance enhancement of a hybrid multi effect evaporation/membrane distillation system driven by solar energy for desalination. *J Environ Chem Eng* 10(6):108855. <https://doi.org/10.1016/j.jece.2022.108855>
- Falih AH, Al Maliki A, Al-lami AK, Jasm A, Mohammed A, Mahmood A, Alameer A, Salah Z, Al-Ansari N, Yaseen ZM (2023) Comparative study on salinity removal methods: an evaluation-based stable isotopes signatures in ground and sea water. *Appl Water Sci* 13(6):1–8
- Goodarzi F, Zendejboudi S (2019) Effects of salt and surfactant on interfacial characteristics of water/oil systems: molecular dynamic simulations and dissipative particle dynamics. *Ind Eng Chem Res* 58(20):8817–8834
- Hamzah N, Nagarajah M, Leo CP (2018) Membrane distillation of saline and oily water using nearly superhydrophobic PVDF membrane incorporated with SiO₂ nanoparticles. *Water Sci Technol* 78(12):2532–2541

- Han L, Tan YZ, Netke T, Fane AG, Chew JW (2017) Understanding oily wastewater treatment via membrane distillation. *J Memb Sci* 539:284–294
- Huang Y-X, Wang Z, Jin J, Lin S (2017) Novel Janus membrane for membrane distillation with simultaneous fouling and wetting resistance. *Environ Sci Technol* 51(22):13304–13310. <https://doi.org/10.1021/acs.est.7b02848>
- Igwe O, Ngwoke M, Ukah BU, Ubido OE (2021) Assessment of the physicochemical qualities of groundwater and soils around oil-producing communities in Afam, area of Porthacourt, Niger Delta Nigeria. *Appl Water Sci* 11:1–13
- Kharraz JA, Farid MU, Jassby D, An AK (2022) A systematic study on the impact of feed composition and substrate wettability on wetting and fouling of omniphobic and janus membranes in membrane distillation. *J Memb Sci* 641:119873
- Maddah HA, Alzhrani AS, Bassyouni M, Abdel-Aziz MH, Zoromba M, Almalki AM (2018) Evaluation of various membrane filtration modules for the treatment of seawater. *Appl Water Sci* 8:1–13
- Mansi AE, El-Marsafy SM, Elhenawy Y, Bassyouni M (2022) Assessing the potential and limitations of membrane-based technologies for the treatment of oilfield produced water. *Alexandria Eng J* 68:787–815
- Mhlanga SD, Tshabalala TG, Nxumalo EN, Mamba BB (2014) Synthesis of PVDF ultrafiltration membranes supported on polyester fabrics for separation of organic matter from water. In: IOP conference series: materials science and engineering, IOP Publishing, p 012036
- Mohammadi Ghalehi M, Al Balushi A, Kaviani S, Tavakoli E, Bavarian M, Nejati S (2018) Fabrication of Janus membranes for desalination of oil-contaminated saline water. *ACS Appl Mater Interfaces* 10(51):44871–44879. <https://doi.org/10.1021/acsami.8b16621>
- Munirasu S, Haija MA, Banat F (2016) Use of membrane technology for oil field and refinery produced water treatment—a review. *Process Saf Environ Prot* 100:183–202
- Olajire AA (2020) Recent advances on the treatment technology of oil and gas produced water for sustainable energy industry-mechanistic aspects and process chemistry perspectives. *Chem Eng J Adv* 4:100049. <https://doi.org/10.1016/J.CEJA.2020.100049>
- Osman MS, Masindi V, Abu-Mahfouz AM (2019) Computational and experimental study for the desalination of petrochemical industrial effluents using direct contact membrane distillation. *Appl Water Sci* 9:1–13
- Rahimi S, Zinatizadeh AA, Mohammadi P, Zinadini S, Asadi A (2020) Performance of an activated sludge followed by membrane process (AS-MP) treating simulated industrial wastewaters: effects of operating factors and feed characteristics. *Appl Water Sci* 10:1–19
- Ricceri F, Giagnorio M, Farinelli G, Blandini G, Minella M, Vione D, Tiraferri A (2019) Desalination of produced water by membrane distillation: effect of the feed components and of a pre-treatment by fenton oxidation. *Sci Rep* 9(1):14964. <https://doi.org/10.1038/s41598-019-51167-z>
- Saber A, Hasheminejad H, Taebi A, Ghaffari G (2014) Optimization of Fenton-based treatment of petroleum refinery wastewater with scrap iron using response surface methodology. *Appl Water Sci* 4:283–290
- Sandid AM, Bassyouni M, Nehari D, Elhenawy Y (2021) Experimental and simulation study of multichannel air gap membrane distillation process with two types of solar collectors. *Energy Convers Manag* 243:114431
- Shi D, Gong T, Qing W, Li X, Shao S (2022) Unique behaviors and mechanism of highly soluble salt-induced wetting in membrane distillation. *Environ Sci Technol* 56(20):14788–14796. <https://doi.org/10.1021/acs.est.2c03348>
- Ye Y, Li T, Zhao Y, Liu J, Lu D, Wang J, Wang K, Zhang Y, Ma J, Drioli E (2023) Engineering environmentally friendly nanofiber membranes with superhydrophobic surface and intrapore interfaces for ultrafast Oil-water separation. *Sep Purif Technol* 317:123885

Publisher's Note Springer Nature remains neutral with regard to jurisdictional claims in published maps and institutional affiliations.